Analysis of the conversion of δ-(L-α-aminoadipoyl)-L-cysteinyl-D-α-aminobutyrate by active-site mutants of *Aspergillus nidulans* isopenicillin N synthase

Christine J Rowe*, Celia P Shorrock, Timothy DW Claridge and John D Sutherland

Background: Penicillins and cephalosporins constitute a major class of clinically useful antibiotics. A key step in their biosynthesis involves the oxidative cyclisation of δ-(L-α-aminoadipoyl)-L-cysteinyl-D-valine to isopenicillin N by isopenicillin N synthase (IPNS). This chemically remarkable transformation has been extensively studied using substrate analogues. The conversion of an analogue in which the valine is replaced by α-aminobutyrate results in three products, two epimeric penams and a cepham. The ratio of these products in reactions catalysed by four different IPNS isozymes has been used previously to probe the thermicity of the chemical mechanism. But how IPNS restricts the products from the natural substrate to a single penam (isopenicillin N) has remained unknown.

Results: A key active-site residue, Leu223, identified according to a model of enzyme–substrate binding, has been altered to sterically less demanding residues. As the steric constraints on the upper part of the active site are reduced, the ratio of the β-methyl penam to the cepham increases when the α-aminobutyrate-containing substrate analogue is used. These results suggest a mechanism for processing of the natural substrate in which IPNS uses steric control to restrict the conformational freedom of an intermediate such that the only product is the penam.

Conclusions: Using steric pressure to control conformation, and hence to disfavour reactions leading to alternate products, is probably the result of evolutionary selection for a biologically active product at the expense of biologically inactive byproducts. It is likely that this sort of enzymatic catalysis is used in situations where substrate conversion is highly exothermic and a variety of products are possible.

Address: The Oxford Centre for Molecular Sciences and The Dyson Perrins Laboratory, South Parks Road, Oxford OX1 3QY, UK.

*Present Address: Department of Biochemistry, University of Cambridge, Tennis Court Road, Cambridge CB2 1QW, UK.

Correspondence: John D Sutherland
E-mail: john.sutherland@chemistry.ox.ac.uk

Key words: biosynthesis, catalysis, penicillin

Received: **30 December 1997**
Revisions requested: **11 February 1998**
Revisions received: **4 March 1998**
Accepted: **6 March 1998**

Published: **15 April 1998**

Chemistry & Biology April 1998, 5:229–239
http://biomednet.com/elecref/1074552100500229

Introduction

A key step in the biosynthesis of penicillins and cephalosporins, which together constitute a major class of antibiotics, is the conversion of δ-(L-α-aminoadipoyl)-L-cysteinyl-D-valine (ACV, **1**) to isopenicillin N (IPN, **2**; see Figure 1) [1,2]. This chemically unusual four-electron oxidative transformation is mediated by isopenicillin N synthase (IPNS), an enzyme that has been the subject of intensive study. When the X-ray crystal structure of *Aspergillus nidulans* IPNS complexed with manganese II ions was solved [3] it did not indicate the mode of substrate binding, so a model was required [4]. The structure revealed four enzyme metal ligands, His214, Asp216, His270 and Gln330. The finding that Gln330, the penultimate residue of the protein, was a metal ligand through its sidechain was unexpected. Other members of the sequence-homologous enzyme family have the two histidine and the aspartate ligands but lack the glutamine ligand. This observation has to be reconciled with the fact that although the other members of the family (for example deacetoxycephalosporin C synthase [5]) bind α-ketoglutarate as an obligate cosubstrate, IPNS does not. Indeed, IPNS must not bind α-ketoglutarate, as IPNS utilizes the full oxidising capacity of dioxygen to convert its substrate ACV **1** to isopenicillin N **2**. This result suggested that IPNS might be using Gln330 as a 'dummy' ligand to prevent α-ketoglutarate from binding [4]. If this is the case, then the dummy ligand must, in some way, be displaced by the ACV **1** substrate but not by α-ketoglutarate. Comparison of the α-aminoadipoyl sidechain of ACV **1** with the carboxy-terminal Gln330–Thr331 tail of IPNS revealed a compelling similarity, which immediately suggested that the selective displacement of the 'dummy' ligand by ACV **1** and not by α-ketoglutarate could occur by structural–functional similarity. In particular, the residues used in binding of the

Figure 1

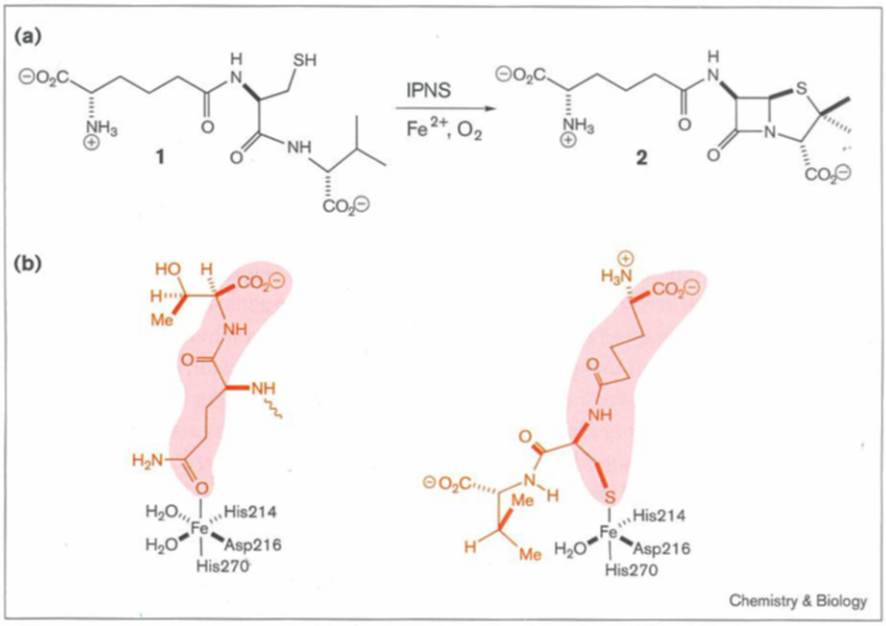

The reaction catalysed by isopenicillin N synthase (IPNS). **(a)** During the oxidative cyclisation of δ-(L-α-aminoadipoyl)-L-cysteinyl-D-valine (ACV, **1**) to isopenicillin N (IPN, **2**), one molecule of dioxygen is reduced to two molecules of water. **(b)** A model for substrate binding (for further discussion see the Introduction section). The first crystal structure of IPNS complexed with manganese II atoms revealed four enzyme metal ligands, His214, Asp216, His270 and Gln330, but did not indicate the mode of substrate binding. Because other enzymes in a sequence-homologous family bind α-ketoglutarate as an obligate cosubstrate and lack the Gln330 metal ligand it was postulated that the Gln330–Thr331 carboxyl terminus of IPNS interacts with the substrate binding site, preventing the binding of α-ketoglutarate in this case. The natural substrate, ACV **1**, is structurally homologous to the Gln330–Thr331 tail, allowing the substrate to displace the tail [4]. IPNS is shown interacting with its carboxy-terminal tail on the left and ACV **1** on the right (both are shown in red, with the portion of the tail/substrate that is essential for interaction with Fe indicated by a pink cloud). Note that Fe interacts non-covalently with the four metal ligands (including Gln330 of the IPNS carboxy-terminal tail) and the two water molecules; the geometry of the interactions is shown.

carboxy-terminal Gln330–Thr331 tail to the protein (principally Arg87 through a salt-bridge to the carboxylate of Thr331 [5]) should also be involved in the binding of the α-aminoadipoyl sidechain of ACV **1**. With this site of attachment of the substrate and the α-aminoadipoyl sidechain in an extended conformation [1], the sulphur atom of the cysteinyl residue of ACV **1** is in an ideal location to ligate the metal. We originally proposed that the sulphur coordinated *trans* to Asp216; the modified coordination shown in Figure 1 derives from subsequent crystallographic data (see below). The predicted binding model [4] then placed the valinyl carboxylate of the substrate close to Arg279 and Ser281, two residues completely conserved in the homology family mentioned earlier. We proposed that the conservation of these two residues reflects the fact that they are used in the binding of α-ketoglutarate in those members of the homology family that use this α-ketoacid as a substrate. In IPNS, α-ketoglutarate binding is prevented by the 'dummy' ligand, so the presence of Arg279 and Ser281 is consistent with our proposal that they function to bind the valinyl carboxylate of ACV **1**. The binding model [4] indicated that the isopropyl group of ACV **1** would be in close proximity to the metal ion and in contact with a number of hydrophobic residues notably Leu223, Pro283, Leu231 and Val272 (see below). The complete conservation of Leu231 in the homology family suggests that this residue is involved in α-ketoglutarate binding in other members of the family. The lack of general acidic and basic residues in this pocket forced us to propose a mechanism in which substrate deprotonation was mediated by an iron-ligated species. This binding model has recently been confirmed by X-ray crystallographic analysis, the only minor difference being that the iron-coordination site is occupied by sulphur [6]. The recent substrate-bound crystal structure shows that the substrate valinyl-C–H bond points away from the iron centre [6]. At some stage of the reaction a rotation of the valinyl-C2–C3 bond must take place to orient the C–H bond towards the metal. Given this fact, and the requirement for the enzyme to stabilise multiple intermediates and transition states, it is apparent that substantial flexibility must be available to the enzyme–substrate complex as the reaction takes place. For this reason it is inappropriate to extrapolate the relative ground-state dispositions of substrate and enzyme to the intermediate states and transition states considered in this paper. This caveat clearly applies to all mechanistic suggestions deriving from ground-state crystal structures.

The chemical mechanism of IPNS has been probed extensively using substrate analogues, and the information gained from these studies, in addition to crystallographic data and comparisons to related enzymes, suggest a detailed mechanism for IPNS (see Figure 2). A key feature of the IPNS mechanism is the oxidative addition of a ferryl oxene (**10**, Figure 2) to the valinyl tertiary C–H bond to give a metallocycle **11** from which reductive elimination generates the product **2**.

Figure 2

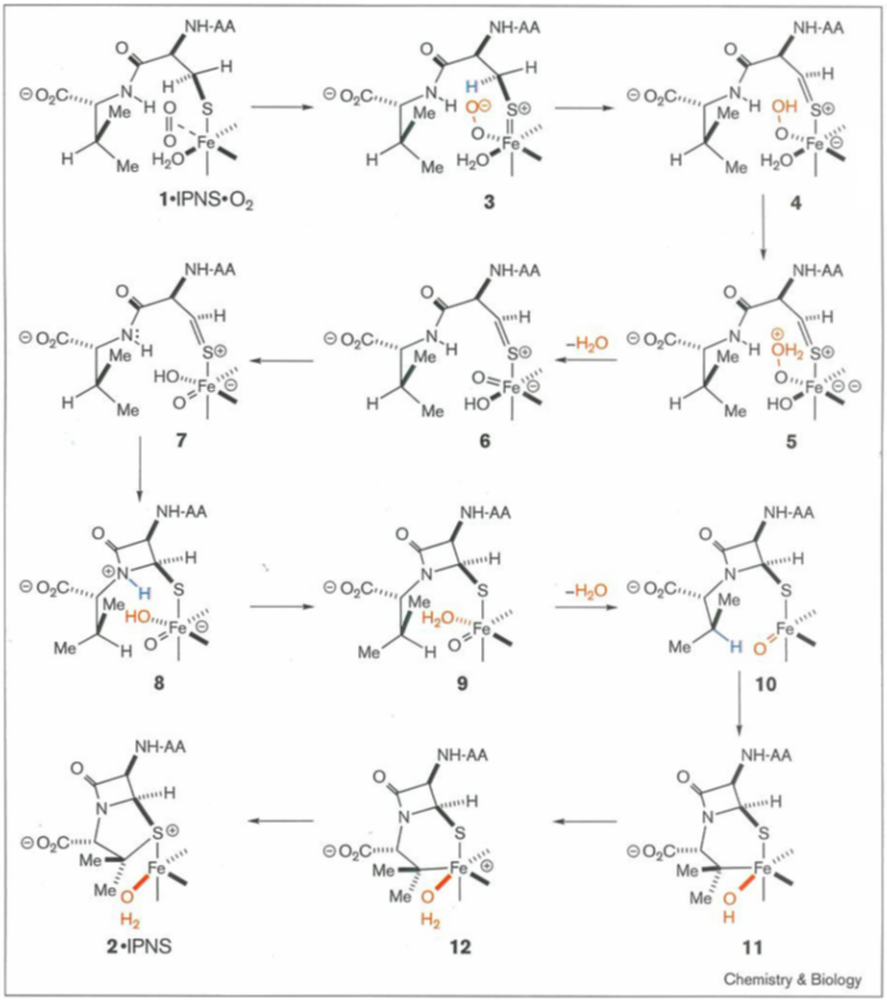

The mechanism of penicillin formation. Binding of the thiolate of the substrate ACV **1** increases electron availability at the ferrous iron, allowing binding of dioxygen. Electron transfer from sulphur to oxygen via the iron generates a peroxy species **3**, in which the non-ligating peroxy oxygen (red) is ideally positioned to function as an intramolecular general base for the abstraction of the cysteinyl-3-*pro*-*S* hydrogen (blue), giving a bound thioaldehyde (**4**). Intracomplex proton transfer gives a peroxy species **5** that is set up to lose water (red), to generate a hydrated ferryl oxene **6**. After proton transfer, the valinyl nitrogen lone pair of **7** can close onto the bound thioaldehyde to give a protonated β-lactam intermediate **8**. Rotation of the valinyl isopropyl group must accompany this ring closure to relieve steric compression. The proton on the valinyl nitrogen (blue) is then removed by the iron hydroxide (red), resulting in intermediate **9**, which loses water again to relieve steric compression. The ferryl oxene of **10** (red) then undergoes a [σ2s+π2a] cycloaddition with the valinyl tertiary C–H bond (blue) to give a metallocyclic intermediate **11**. After solvent-mediated iron hydroxide protonation, reductive elimination from **12** generates the enzyme-bound product (IPN, **2**).

The study of one substrate analogue has been particularly revealing; δ-(L-α-aminoadipoyl)–L-cysteinyl–D-α-aminobutyrate (ACAB, **13**, which lacks one of the methyl groups of the natural substrate) is converted to three products, the β-methyl penam **20**, the α-methyl penam **21** and the cepham **22**, by IPNS (see Figure 3) [7,8]. Comparing the ratios of these three products from the conversion of ACAB **13** by four different IPNS isozymes enabled several conclusions to be drawn [9]. The invariance of the ratio of combined penam products to the cepham, (**20**+**21**):**22**, suggested, by applying Hammond's postulate [10], that the chemical step that discriminates between the penams and the cepham is highly exothermic. The minor perturbations caused by sequence differences between the isozymes do not affect the product ratio (**20**+**21**):**22** because ground-state binding differences are reflected by very similar transition-state differences. On the other hand the ratio of β- to α-methyl penams, **20**:**21**, was found to be significantly variable implying that the step that discriminates between the two penams is less exothermic such that the perturbations affect ground-state-and transition-state-binding differentially. The results of this heuristic analysis were interpreted according to a reaction scheme based on three conformational states (see Figure 3). Two-electron oxidation of ACAB **13** produces a monocyclic ferryl-oxene intermediate that can exist in three conformational states about the α-aminobutyrate C2–C3 bond, the 'methyl-up' conformer **14**, the 'methyl-left' conformer **15** and the 'methyl-right' conformer **16**. Oxidative insertion of the ferryl-oxene moiety into a C–H bond of these conformers produces the metallocyclic intermediates **17**, **18** and **19**, from **14**, **15** and **16**, respectively. The oxidative addition step discriminates between the formation of penam and cepham products and was suggested by our analysis to be highly exothermic, in accordance with chemical expectations. The monocyclic ferryl oxene intermediate must have a significant lifetime, however, because the overall reaction is sensitive to substrate deuteration at the valinyl/α-aminobutyryl-3-position [2],

Figure 3

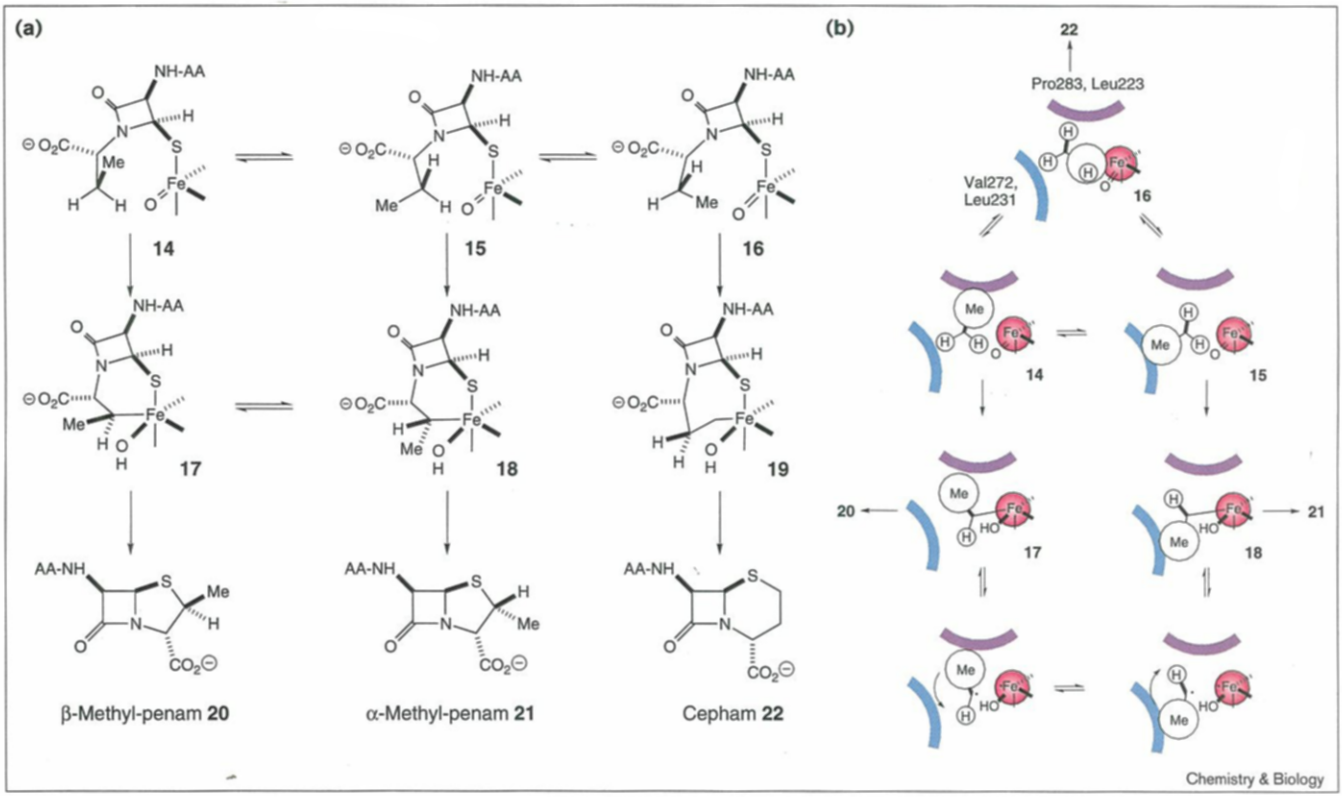

Processing of an ACV analogue by IPNS. **(a)** The mechanism of conversion of δ-(L-α-aminoadipoyl)–L-cysteinyl–D–α-aminobutyrate (ACAB **13**) by IPNS [7,8]. Three conformers at the ferryl oxene stage (**14**, **15** and **16**) undergo cycloaddition to give the metallocyclic intermediates **17**, **18** and **19** (**17** and **18** can interconvert by way of a diradical intermediate). Reductive elimination then generates the β-methyl-penam (**20**), α-methyl-penam (**21**) and cepham (**22**) products. **(b)** Schematic representation of the chemistry portrayed in (a). The chemistry takes place in a hydrophobic pocket created by the isopropyl methyl groups of Leu231 and Val272 at the lower left (blue) and the sidechains of Leu223 (again the isopropyl methyl groups) and Pro283 at the top (purple). The relative ground-state positions of these residues are not indicated, as there must be small but significant changes throughout the reaction cycle. The general disposition of the residues comprising the hydrophobic pocket is unlikely to change, however. Accordingly, the general area occupied by these residues is shown by the coloured surfaces in this and subsequent figures. The iron centre (pink) imposes an additional steric constraint on binding. The metallocyclic intermediates leading to the two penam products can interconvert through the intermediacy of a freely rotating diradical [8].

suggesting that, although the oxidative addition is highly exothermic, there is a high, rate-determining barrier that must be overcome. The oxidative addition step is therefore a good candidate for positive catalysis by the enzyme. Deuteration of the 3-position of valine in ACV **1** leads to the formation of small amounts of a shunt metabolite, suggesting that the 'wrong' chemistry is somehow disfavoured at the stage of the monocyclic ferryl oxene intermediate. The metallocycle **19** (possibly in equilibrium with a diradical) can then undergo reductive elimination to give the cepham **22**. Isotopic labelling studies clearly indicate the interconversion of the two six-membered metallocycles **17** and **18** presumably through a freely rotating diradical [8]. The event that discriminates between the two penam products is the reductive elimination to give the β- and α-methyl penams **20** and **21**, from **17** and **18** respectively. The comparative analysis suggested that the reductive elimination step is less exothermic than the oxidative addition step, and the fact that stereochemical interconversion through the intermediacy of the diradical is possible [8] also suggests that the metallocycles **17** and **18** (and, by inference, **19**) must have significant lifetimes.

We have been interested in assessing the ways in which IPNS catalyses the complicated chemistry of this reaction and the way in which such an enzyme might have evolved. In particular, we seek to explain why other products that might potentially arise from the oxidative processing of ACV **1** are not observed (for example, cephams deriving from addition of the ferryl oxene to primary C–H bonds of the methyl groups of **1**). In this paper, we report results with active-site mutants of IPNS that shed new light on these issues.

Figure 4

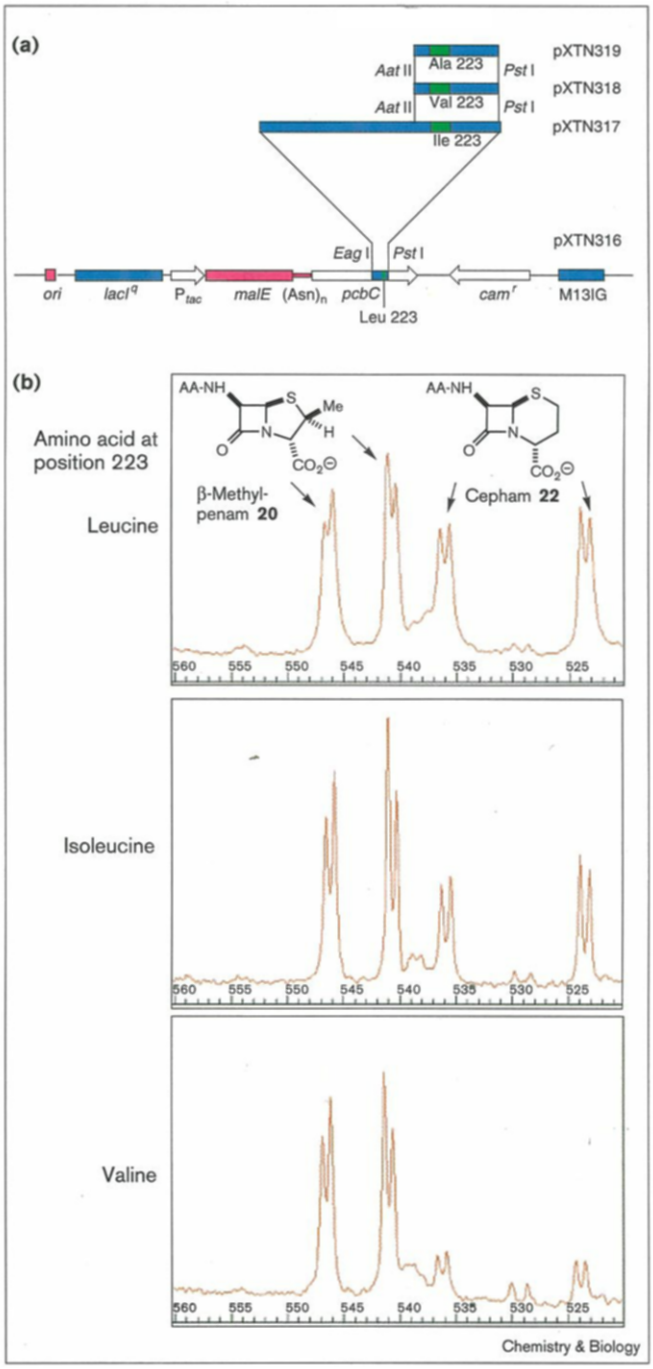

aIPNS mutants used in this study. **(a)** Construction of vectors encoding the IPNS mutants; pXTN316 was constructed by subcloning the *Aspergillus nidulans pcbC* gene [11] encoding aIPNS into a chloramphenicol-resistant derivative of pMal-c2. Introduction of a synthetic cassette containing an *Aat*II site into pXTN316/*Eag*I, *Pst*I gave pXTN317 (Leu223→Ile). Introduction of smaller synthetic cassettes into pXTN317 cleaved by *Aat*II and *Pst*I then gave pXTN318 (Leu223→Val) and pXTN319 (Leu223→Ala). **(b)** Product distribution from the conversion of the substrate analogue ACAB **13** by the wild-type IPNS and Leu223→Ile and Leu223→Val active-site mutants.

Results and discussion

Given the analysis of the conversion of ACAB **13** by IPNS, we reasoned that our novel binding model could be tested by mutating Leu223 to other residues that would alter the steric demands of the ACV-binding pocket; in addition the effect of these mutations on the product ratios would provide further mechanistic information about IPNS.

Recombinant *Aspergillus nidulans* IPNS (pcbC/aIPNS) was selected as the isozyme for our mutagenesis experiments because the expression levels, purification and stability are better than for the recombinant isozymes from *Cephalosporium acremonium*, *Streptomyces lipmanii* and *Penicillium chrysogenum* [11]. Because we envisaged an extensive series of mutagenesis experiments, we decided to construct a vector expressing a fusion protein that could be rapidly purified using affinity chromatography. Maltose-binding protein (MalE) was selected as the fusion partner and a vector, pXTN316, suitable for cassette mutagenesis of the Leu223 region was constructed (see Figure 4) [3]. Expression of the *malE–pcbC* fusions yielded large amounts of the wild-type and mutant fusion proteins that were conveniently purified using gel-filtration chromatography or affinity chromatography on amylose eluting with maltose-containing buffers. Incubation experiments with the IPNS mutants and ACV **1** or ACAB **13** were conducted side-by-side under identical conditions. Products were analysed using ^{1}H nuclear magnetic resonance (NMR) spectroscopy (D_2O, 500MHz). Experiments in which the wild-type fusion protein was compared to unfused IPNS revealed that kinetic parameters were unaffected by the presence of the maltose-binding protein, other than the effect of increased molecular weight. With ACV **1**, a progressive decrease in specific activity was observed as Leu223 was changed to isoleucine, valine or alanine. In all cases, however, the only β-lactam product detected was the normal product (IPN, **2**), and no cephams (for which synthetic standards were available) were detected. Conversions of ACAB **13** by the Leu223→Ala mutant were very low and are not considered further here except to say that the trend in favour of the β-methyl penam **20** was continued. The results of conversion of ACAB **13** by the other IPNS mutants are shown in Figure 4.

As is evident from Figure 4, decreasing the steric demand of the sidechain of residue 223 alters the products, increasing the amount of β-methyl penam **20** relative to the cepham **22**. Under the conditions of the experiment, the α-methyl penam **21** was only just detectable with the wild-type fusion and was not detected in experiments using the Leu223→Ile or Leu223→Val mutants. In contrast to our earlier results using different isozymes [11], the penam: cepham ratio is clearly altered by mutagenic perturbation in this case. With wild-type IPNS (pXTN316), the ratio of β-methyl penam **20** to cepham **22** was 1:1, with the Leu223→Ile mutant (pXTN317) the ratio was 3:2 and

Figure 5

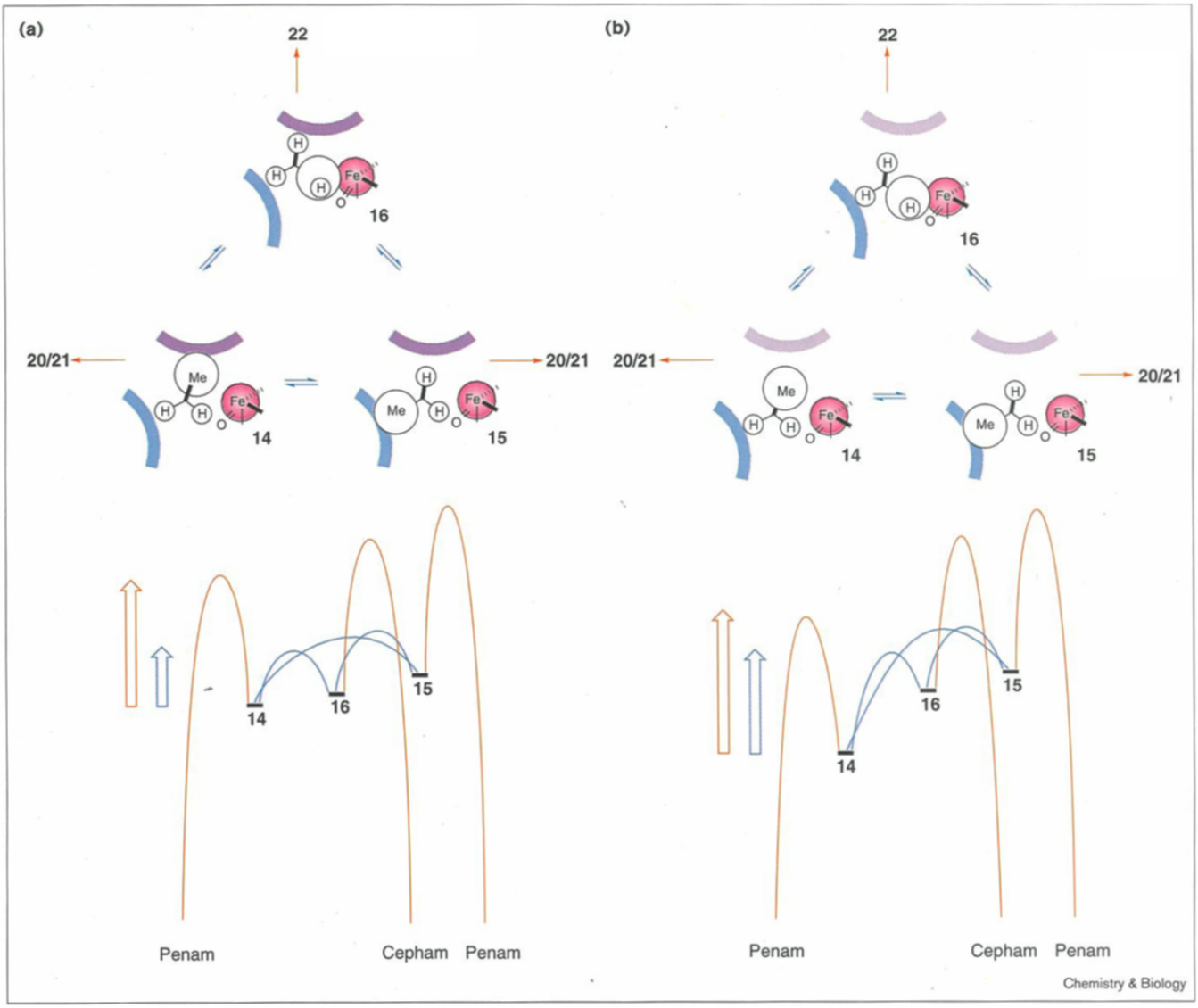

The effect of active-site mutations on the energetics of processing ACAB **13** by aIPNS. **(a)** Energetics of rotation and oxidative addition for wild-type IPNS and ACAB **13**. Conformational energy barriers (blue) are considerably lower than the corresponding barriers for oxidative addition (red). **(b)** Energetics of rotation and oxidative addition for the isoleucine and valine IPNS active-site mutants and ACAB **13**.

with the Leu223→Val mutant (pXTN318) the ratio 3:1. An explanation for these observations can be provided with reference to Figures 5 and 6.

The previous analysis [9] strongly suggested that the oxidative addition reaction is relatively exothermic. As a consequence of the Hammond postulate, any minor perturbation that stabilises or destabilises one of the conformational states **14**, **15** or **16** would similarly stabilise or destabilise the transition-state leading from that particular conformer. Because the three conformers **14**, **15** and **16** can rotate with energy barriers lower than those for the subsequent oxidative addition, the Curtin–Hammett principle [12] prevails. The penam:cepham ratio is therefore governed solely by the relative heights of the energy barriers for the respective oxidative additions. The heights of these barriers are not changed by minor perturbations and the ratio of penams **20** and **21** to cepham **22** remains essentially constant. The active-site mutations studied here constitute major perturbations of IPNS, however, and result in the upper part of the enzyme's hydrophobic pocket being less sterically demanding. The consequent increase in the stability of conformer **14** relative to conformers **15** and **16** results in the activation

Figure 6

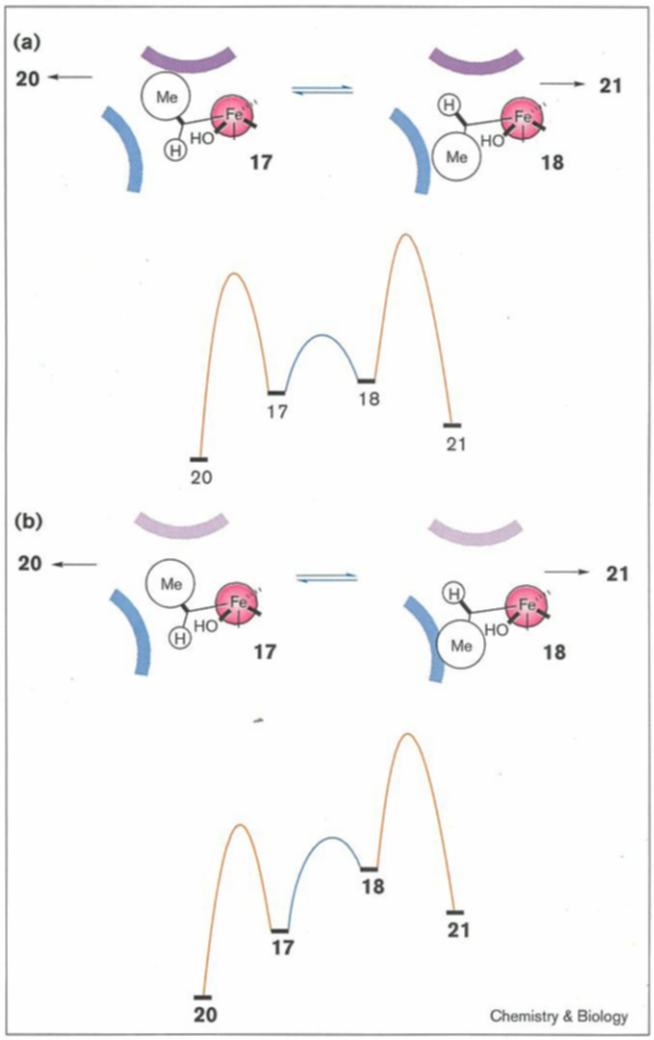

The effect of active-site mutations on the energetis of the α/β-methyl penam discriminating step. **(a)** Energetics for interconversion of (blue) and reductive elimination from (red) metallocyclic intermediates **17** and **18** with wild-type IPNS. **(b)** Corresponding energetics for the isoleucine and valine IPNS active-site mutants.

barrier to rotation about the α-aminobutyryl-C2–C3 bond being increased to the extent that it is comparable to the activation barrier for oxidative addition. At this point, the Curtin–Hammett principle no longer prevails and the ratio of penams **20** and **21** to cepham **22** increases.

The stabilisation of conformer **14** relative to conformers **15** and **16** could be caused in two ways; either conformer **14** could be stabilised or conformers **15** and **16** could be destabilised. It seems unlikely that mutations that create more space in the active site could destabilise conformer **16**, which suffers from steric interactions between the methyl group and the ferryl oxene moiety, so it seems likely that the mutations act by stabilising the 'methyl-up' conformer **14**. If, in the wild-type, Leu223 was involved in an ideal van der Waals contact with a substrate methyl group in the 'up' position, then changing Leu223 to a sterically less demanding residue would not increase the degree of stabilisation — rather, it should decrease it. It is thus necessary to conclude that, in the wild-type, the fit between Leu223 and a methyl group in the 'up' position is too tight to be stabilising and is, in fact, unfavourable. The fact that processing of ACAB **13** by wild-type IPNS gives roughly comparable amounts of β-methyl penam **20** and cepham **22** when Leu223 destabilises the 'methyl-up' conformer **14** implies that the 'methyl-right' conformer **16** must be equally unfavoured. Similar arguments suggest that the 'methyl-left' conformer **15** must be the most disfavoured of the three rotamers. The steric pressure on the methyl group of the 'methyl-left' **15** conformer appears to be caused by the hydrophobic residues Leu231 and Val272. Experiments to investigate the effects of mutating these residues are now in progress. Thus occupancy of the three conformational states at the monocyclic ferryl oxene stage during ACAB **13** processing is dictated by the methyl group occupying the two least bad positions. The penam:cepham ratio is determined by the effect these conformational preferences have on the oxidative addition step.

The relative amounts of the two penams (**20**, **21**) are determined at the later stage of reductive elimination (see Figure 6). The reductive elimination is not as exothermic as the oxidative addition step so, according to Hammond's postulate, the transition states for reductive elimination respond to minor perturbation differently than do the metallocycles. The ratio of **20** to **21** using the different IPNS isozymes is therefore variable [9]. The preference for production of the β-methyl-penam **20** indicates that the barrier leading to **20** is lower than the barrier leading to **21**. Given the nature of the hydrophobic pocket, it is likely that the metallocycle **17**, β-methyl penam **20** and the transition state in between are all lower in energy than the corresponding states leading to the α-methyl penam **21**. In the case of the IPNS active-site mutants, stabilization of **17** relative to **18** means that the height of the interconversion barrier is comparable to the height of the reductive elimination barriers. Because of the reduced exothermicity of the reductive elimination step, the transition state between **17** and **20** will be differentially stabilised relative to **17** by the mutant enzymes mutations. Because the reductive elimination involves the methine carbon migrating from the ferryl centre to the cysteinyl-derived sulphur atom, the decreased steric bulk in this region should result in the transition state for the shift being preferentially stabilised, relative to **17**. Therefore the β-methyl penam **20** predominates.

In the case of the the natural substrate, ACV **1**, an argument can now be put forward to explain the lack of

Figure 7

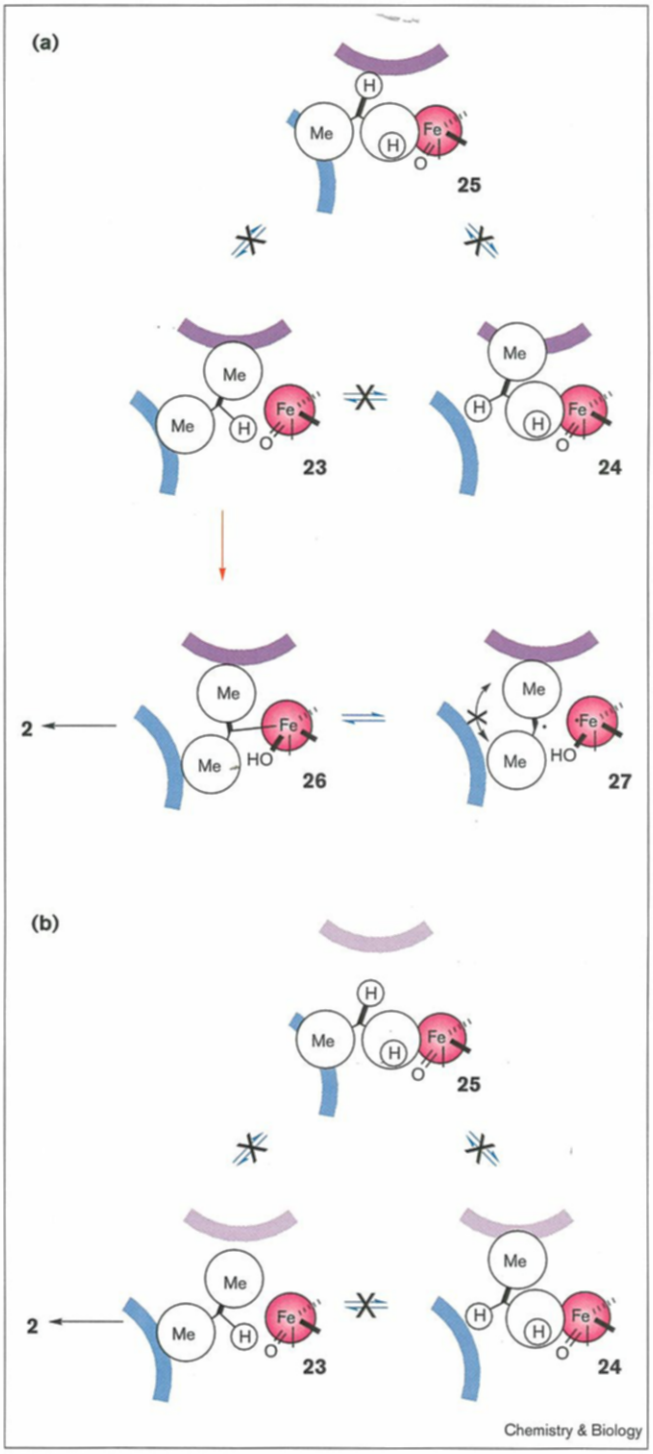

Schematic representation of the role of steric control of conformation in the reaction of **(a)** ACV 1 with wild-type IPNS and **(b)** with the isoelucine and valine active-site mutants.

cepham products in the reaction catalysed by wild-type IPNS (see Figure 7). The extra methyl group in the natural substrate **1** (relative to ACAB **13**) means that the two possible conformations (**24** and **25**) leading to cepham products both suffer from two severely unfavourable interactions (**24** is unavailable because of pressure from the iron centre and from above, **25** is unavailable because of pressure from the iron centre and from below left). The least disfavoured conformation (**23**) is therefore the only available state. The steric pressure exerted on conformer **23** is partly relieved upon oxidative addition to give the metallocycle **26**; the oxidative addition step is therefore catalysed by steric effects. Equilibration of the metallocycle **26** with the diradical **27** is assumed possible (the carbon-centred radical is tertiary) but isotopic labelling results rule out free rotation of this diradical [13]; presumably the extra methyl group in **1** relative to **13** results in the energetic barrier for free rotation of **27** also being unsurmountable. Reductive elimination from **26** then generates bound product **2**. In the case of the mutant enzymes, the two conformational states (**24** and **25**) leading to cepham products are still disfavoured and product **2** results from oxidative addition to give conformer **23**. The reduced steric pressure results in this being a less efficient reaction than with the wild-type enzyme, however. It remains to be seen whether the diradical **27** can rotate in the mutant enzymes, which is now clearly a possibility.

In summary, the results and analysis presented here indicate the extent to which IPNS has evolved to use steric control of conformation as a way to mediate catalysis (see Figure 8). Further reduction of steric pressure by active-site mutagenesis is likely to result in cepham products (most likely the β-methyl cepham **31**) and increased amounts of the shunt metabolite **28** (formed via the intermediacy of **29** when the ferryl oxene is allowed to persist). It seems likely, therefore, that primitive IPNS enzymes produced more than one product (for example, hydroxylation products can be derived from a high energy species such as **10**). Evolutionary selection for the production of **2** would then have provided the pressure for the use of steric control to decelerate processes leading to unuseful products and to accelerate the process leading to **2**.

Significance

The oxidative cyclisation of δ-(L-α-aminoadipoyl)-L-cysteinyl-D-valine to isopenicillin N by isopenicillin N synthase (IPNS) is a key step in the biosynthesis of an important class of antibiotics comprising the penicillins and cephalosporins. A combination of X-ray crystallography and the use of substrate analogues has gone a long way towards explaining the mechanistic basis of this chemically remarkable transformation. Because the first crystal structure of IPNS [3] did not indicate the mode of substrate binding, we generated a model for substrate binding [4]. We postulated that the natural substrate of IPNS interacted with four residues at the

Figure 8

The likely development of steric control of conformation as a means of maximising the yield of a biologically active product at the expense of biologically inactive by-products. See text for further details.

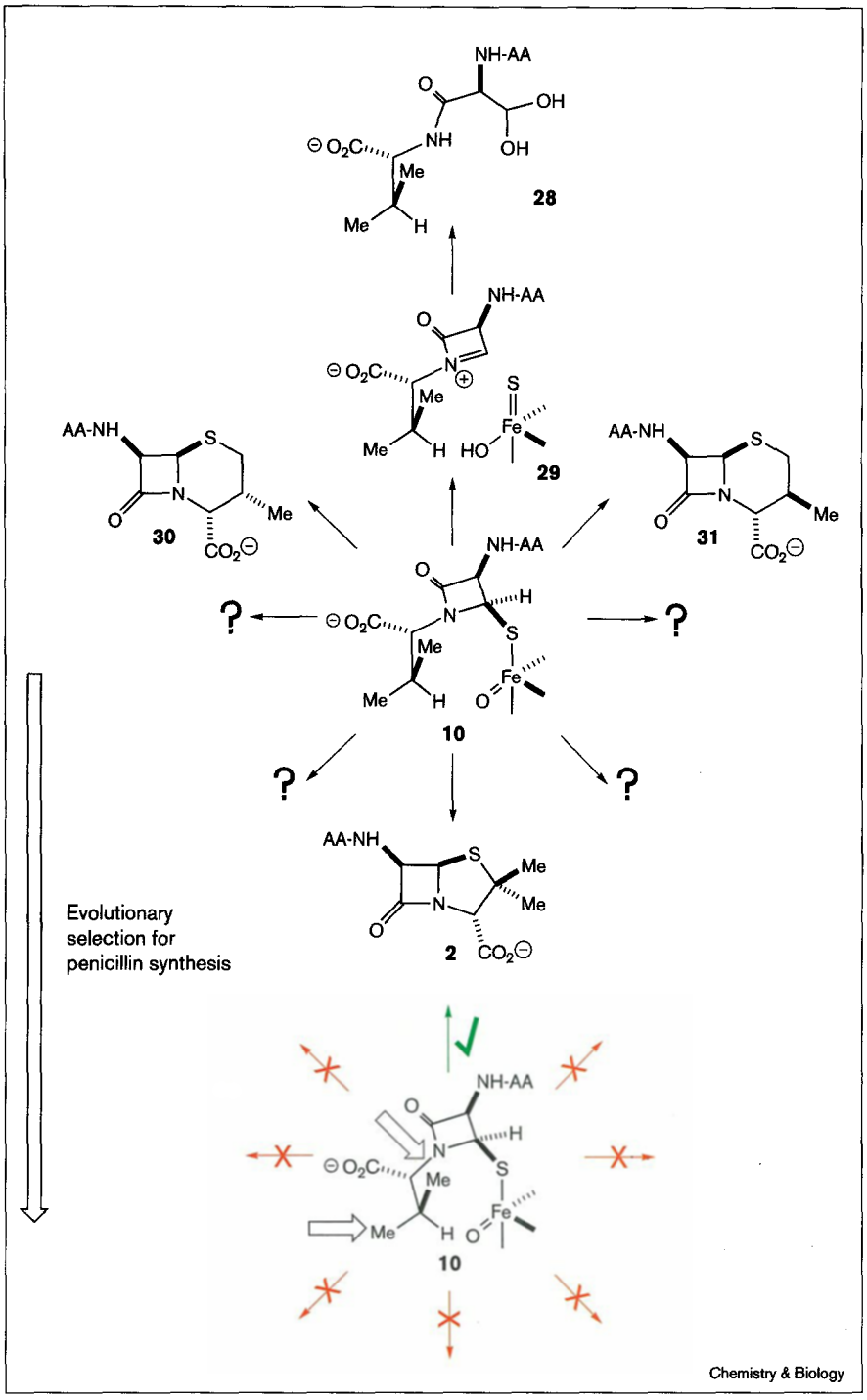

active site — Leu223 and Pro283 at the 'top' of the active site and Leu231 and Val272 below. This was confirmed by a more recent structure [6]. To further investigate the mechanism of IPNS, we increased the size of the active-site cavity above the substrate by mutating Leu223 to isoleucine, valine or alanine. The ratio of β-methyl penam to cepham products from the processing of the substrate analogue δ-(L-α-aminoadipoyl)-L-cysteinyl-D-α-aminobutyrate increased as the cavity was made larger (when IPNS processes its natural substrate only one product — a penam — is generated). These results are interpreted in terms of the enzyme exerting steric control of conformation of the natural substrate to prevent the formation of otherwise

likely products. This aspect of enzymic catalysis is important for those exothermic enzyme-catalysed reactions in which several products are possible and only one is selected for evolutionarily.

Materials and methods

General details

^{1}H–NMR spectra were recorded on a Bruker AMX500 (500MHz) spectrometer equipped with a 3 mm Nalorac microprobe and the solvent signal (D_2O) was used as an internal reference. High performance liquid chromatography (HPLC) purifications were carried out on a Gilson HPLC system equipped with Gilson 305 and 306 pumps, a variable wavelength detector, an 806 manomeric module and a model 231 Biosample injector. HPLC instrument control, data collection and analysis were performed on an IBM PS1 model 486DX-33 computer equipped with Microsoft Windows v.3.3 and Gilson 715 v.1.2 software, connected via a Gilson 621 interface module. Reverse-phase HPLC was carried out using a C_{18} Hypersil™ or a Microsorb™ C_{18} column.

Reagents and enzymes

δ-(L-α-Aminoadipoyl)–L-cysteinyl–D-valine (ACV) **1** was a generous gift of Glaxo (now Glaxo-Wellcome Plc, Stevenage, UK). δ-(L-Aminoadipoyl)–L-cysteinyl–D-(α-aminobutyrate) (ACAB) **13** was prepared according to literature procedures [7] and purified using reverse-phase HPLC.

Restriction endonucleases and appropriate 10× buffer concentrates were purchased form Pharmacia and New England Biolabs. Chloramphenicol was purchased from Sigma. IPTG was purchased from Novabiochem. Molecular weight markers for protein and DNA gels were purchased from Gibco-BRL. Sequenase 2.0 for DNA sequencing was purchased in kit form from USB. Deoxynucleotide α-^{35}S-thiotriphosphates were purchased from Amersham International.

Amylose resin for affinity chromatography purification of maltose binding protein fusions was purchased from New England Biolabs. Sephadex G-25 PD-10 columns for gel filtration chromatography and Sephadex G-25 Nap-5 columns for buffer exchange operations were purchased from Phamacia Biotech.

Bacterial strains and DNA

XL1-Blue (*recA*1, *endA*1, *gyrA*96, *thi*1, *hsdR*17, *supE*44, *reclA*1, *lac*, (F'*pro*AB, *lacI*^{q}, *lacZ*^{3}M15, *Tn*10 (tet^r)) and NM554 (*recA*1, *araD*139, ^{3}(*araABC-leu*) 7697, ^{3}*lacX*74, *galU*$^-$, *gal* K$^-$, *hsd* R, *hsd* M$^+$, *rspL*, *strA*, *thi*, *mcrA*(–), *mcrB* (–)) strains of *E. coli* were used. Bacteria were grown at 27°C in Luria-Bertani medium (LB) or on plates. Chloramphenicol (30 μg ml^{-1}) was used as an antibiotic supplement.

Oligonucleotides were synthesized with a Beckman Oligo 1000 DNA synthesizer on a 30 nM scale.

Construction of mutants

pXTN316 was constructed by subcloning the *Aspergillus nidulans pcbC* gene [11] encoding IPNS into a chloramphenicol-resistant derivative of pMal-c2 (pAJL105). Introduction of a synthetic cassette containing an *Aat*II site and the Leu223→Ile mutation into pXTN316/*Eag*I, *Pst*I gave pXTN317. Introduction of smaller synthetic cassettes into pXTN317/*Aat*II, *Pst*I then gave pXTN318 (223→Val mutation) and pXTN319 (223→Ala mutation).

Expression of wild-type aIPNS and mutant aIPNS

E. coli. strain NM554 was transformed with the appropriate plasmid. Transformation mixtures were plated at 27°C onto LB agar containing chloramphenicol (30 μg ml^{-1}). Single colonies were used to inoculate 5 ml of LB containing chloramphenicol (30 μg ml^{-1}) and the cultures were grown overnight at 27°C and 250 rpm. The overnight cultures were used as 1% inocula into 100 ml of LB media containing chloramphenicol (30 μg mL^{-1}). Cultures were incubated at 27°C. When the OD_{600} was between 0.4 and 0.6 IPTG was added to the cultures to a final concentration of 0.5 mM. Cells were harvested by centrifugation at 3500 rpm and lysed by sonication. Soluble lysates were analysed by sodium dodecyl sulphate–polyacrylamide gel electrophoresis (SDS–PAGE). The wild-type IPNS vector pXTN313 yielded MBP:IPNS as ~45% of the total soluble protein, IPNS mutant vector pXTN317 yielded ~40% and pXTN318 and pXTN319 both yielded ~30%.

Purification of wild-type aIPNS and mutant aIPNS

Expression of the *malE:pcbC* fusions yielded large amounts of the wild-type and mutant fusion proteins which were conveniently purified using gel-filtration chromatography on Sephadex G-25 M PD-10 column or affinity chromatography using an amylose resin and eluting with maltose-containing buffers. Purified protein was quantified using the method of Bradford and the specific activities of wild-type and mutant aIPNS were measured by plate bioassay and HPLC assay on a reverse-phase column.

Incubation of δ-(L-α-aminoadipoyl)–L-cysteinyl–D-valine (ACV) **1** and δ-(L-α-aminoadipoyl)–L-cysteinyl–D-(α-aminobutyrate) (ACAB) **13** with wild-type and mutant aIPNS

Protein samples were thawed and buffer exchanged into 50 mM NH_4HCO_3 on a Sephadex G-25 Nap-5 column immediately prior to use. One milligram of ACV **1** or ACAB **13** was dissolved in 200 μl of buffer and 200 μl each of 100 mM dithiothreitol (DTT), 44 mM ascorbate and 1 mM Fe_2SO_4 (all made up in water) were added. This substrate and cofactor mix was added to the enzyme preparation in a round bottom glass flask and the reaction mixture was incubated for 30 min at 27°C and 250 rpm in a bench-top orbital shaker. Cold acetone ~4°C was added to 70% by volume, and the protein was precipitated for 5 min at room temperature. Precipitated protein was removed by centrifugation at 13500 rpm for 5 min and the acetone then removed on a vacuum centrifuge. The aqueous remainder was frozen and lyophilized. The lyophilisate was dissolved in 200 μl of D_2O passed through a sterile 0.22 μm filter and the ^{1}H–NMR spectrum was examined for the presence of characteristic β-lactam resonances in the region of δ4.8–6.0 ppm. All incubations showed a total conversion of the substrate except for the pXTN319 mutant with ACAB **13**. The β-lactam resonances observed were assigned on the basis of ^{1}H–NMR spectra of previously purified metabolites, as detailed below.

Incubation of ACV **1**: (2S,5R,6R)-6-[(5S)-5-Amino-5-carboxypentanamido]-3,3-dimethyl-7-oxo-1-aza-4-thiabicyclo[3.2.0]heptane-2-carboxylic acid (IPN) **2** δH (500 MHz, D_20), 5.35 and 5.45 (2H, ABq, J 4 Hz, 5-H and 6-H).

Incubation of ACAB ***13***: (2S,3S, 5R,6R)-6-[(5S)-5-Amino-5-carboxypentanamido]-3-methyl-7-oxo-1-aza-4-thiabicyclo [3.2.0] heptane-2-carboxylic acid (β-methyl penam **20**) δ_H (500 MHz, D_20), 5.31 and 5.37 (2H ABq, *J* 4 Hz, 5-*H*, 6-*H*). (2S,3R, 5R,6R)-6-[(5S)-5-Amino-5-carboxypentanamido]-3-methyl-7-oxo-1-aza-4-thiabicyclo [3.2.0]heptane-2-carboxylic acid (α-methyl penam **21**) δ_H (500 MHz, D_20), 5.36 and 5.45 (2H ABq, *J* 4Hz, 5-*H*, 6-*H*). (2S,6R,7R)-7-[(5S)-5-Amino-5-carboxypentanamido]-8-oxo-1-aza-5-thiabicyclo[4.2.0]octane-2-carboxylic acid (Cepham **22**) δ_H (500 MHz, D_20), 5.15 and 5.28 (2H, ABq, *J* 4Hz, 6-*H* and 7-*H*).

Analysis of substrate conversions

Incubation of wild-type aIPNS and the several mutant aIPNS with ACV **1** showed in each case a total conversion to a single product, IPN **2**. The specific activity decreased when Leu223 was changed in to isoleucine (pXTN317), valine (pXTN318) or alanine (pXTN319). Incubation of wild-type aIPNS and mutant aIPNS with ACAB **13** showed a total conversion into two main products, β-methyl penam **20** and cepham **22**, except for the Leu223→Ala mutant (pXTN319) which gave very low conversions and is not considered here. The product distribution was affected by the catalyst. With the wild-type IPNS (pXTN316) the ratio of β-methyl penam **20** to cepham **22** was 1:1, with the Leu223→Ile mutant (pXTN317) the ratio was 3:2 and with the Leu223→Val mutant (pXTN318) 3:1.

Acknowledgements

We thank Steve Martin (Glaxo-Wellcome, Stevenage), Jonathan Blackburn, Darren Hart (Cambridge University), Roel Bovenberg, Jan-Metske van der Laan and Dick Schipper (Gist-brocades, Delft) for helpful comments and advice and John Keeping for excellent technical assistance. This work was funded by the UK Research Councils through the OCMS; C.P.S. thanks the Berrow Foundation for studentship support.

References

1. Baldwin, J.E. & Abraham, E.P. (1988). The biosynthesis of penicillins and cephalosporins. *Nat. Prod. Rep.* **5**, 129-145.
2. Baldwin, J.E. & Bradley, M. (1990). Isopenicillin N synthase: mechanistic studies. *Chem. Rev.* **90**, 1079-1088.
3. Roach, P.L., *et al.*, & Baldwin, J.E. (1995). Crystal structure of isopenicillin N synthase is the first from a new family of enzymes. *Nature* **375**, 700-704.
4. Rowe, C.J. (1995). *Genetic Engineering of Penicillin Biosynthesis.* Ph.D. thesis,. Oxford Univeristy, Oxford.
5. Morgan, N., *et al.*, & Sutherland, J.D. (1994). Substrate specificity of recombinant *Streptomyces clavuligerus* deacetoxycephalosporin C synthase. *Bioorg. Med. Chem. Lett.* **4**, 1595-1600.
6. Roach, P.L., *et al.*, & Baldwin, J.E. (1997). Structure of isopenicillin N synthase complexed with substrate and the mechanism of penicillin formation. *Nature* **387**, 827-830.
7. Baldwin, J.E., *et al.*, & Usher, J.J. (1983). Penicillin biosynthesis. Dual pathways from a modified substrate. *J. Chem. Soc. Chem. Commun.*, 1317-1319.
8. Baldwin, J.E., *et al.*, & Usher, J.J. (1983). Penicillin biosynthesis. On the stereochemistry of carbon–sulphur bond formation with modified substrates *J. Chem. Soc. Chem. Commun.*, 1319-1320.
9. Blackburn, J.M., Sutherland, J.D. & Baldwin, J.E. (1995). A heuristic approach to the analysis of enzymic catalysis: Reaction of δ-(L-α-aminoadipoyl)–L-cysteinyl–D-α-aminobutyrate and δ-(L-α-aminoadipoyl)–L-cysteinyl–D-allylglycine catalyzed by isopenicillin N synthase isozymes. *Biochemistry* **34**, 7548-7562.
10. Hammond, G.S. (1955). A correlation of reaction rates. *J. Am. Chem. Soc.* **77**, 334-338.
11. Baldwin, J.E., Blackburn, J.M., Sutherland, J.D. & Wright, M.C. (1991). High-level soluble expression of isopenicillin N synthase isozymes in *E. coli. Tetrahedron* **47**, 5991-6002.
12. Eliel, E.L. (1954). *Stereochemistry of Carbon Compounds.*, McGraw-Hill, New York.
13. Baldwin, J.E., Adlington, R.M., Domayne-Hayman, B.P., Ting, H.-H. & Turner, N.J. (1986). Stereospecificity of carbon–sulphur bond formation in penicillin biosynthesis. *J. Chem. Soc. Chem. Commun.*, 110-113.

Because *Chemistry & Biology* operates a 'Continuous Publication System' for Research Papers, this paper has been published via the internet before being printed. The paper can be accessed from http://biomednet.com/cbiology/cmb – for further information, see the explanation on the contents pages.